Tear Film Lipid Layer Structure : Self-Assembly of O-Acyl-omega-hydroxy Fatty Acids and Wax Esters into Evaporation-Resistant Monolayers

Viitaja, Tuomo

2021-09-22

Viitaja , T , Moilanen , J , Svedström , K J , Ekholm , F S & Paananen , R O 2021 , ' Tear Film Lipid Layer Structure : Self-Assembly of O-Acyl-omega-hydroxy Fatty Acids and Wax Esters into Evaporation-Resistant Monolayers ' , Nano Letters , vol. 21 , no. 18 , pp. 7676-7683 . https://doi.org/10.1021/acs.nanolett.1c02475

http://hdl.handle.net/10138/335023
https://doi.org/10.1021/acs.nanolett.1c02475

NANO LETTERS

pubs.acs.org/NanoLett Letter

Tear Film Lipid Layer Structure: Self-Assembly of *O*-Acyl-ω-hydroxy Fatty Acids and Wax Esters into Evaporation-Resistant Monolayers

Tuomo Viitaja, Jukka Moilanen, Kirsi Johanna Svedström, Filip S. Ekholm,* and Riku O. Paananen*

Cite This: *Nano Lett.* 2021, 21, 7676–7683 Read Online

ACCESS | Metrics & More | Article Recommendations | Supporting Information

ABSTRACT: In healthy eyes, the tear film lipid layer (TFLL) is considered to act as an evaporation resistant barrier, which prevents eyes from drying. Seeking to understand the mechanisms behind the evaporation resistance of the TFLL, we studied mixtures of lipid layer wax esters and *O*-acyl-ω-hydroxy fatty acids. Analyzing their self-assembly and biophysical properties led to new discoveries concerning the structure and function of the TFLL. We discovered how these lipids self-assemble at the air−water interface and form an efficient antievaporative barrier, demonstrating for the first time how the interaction of different tear film lipid species can improve the evaporation resistance compared with individual lipid classes on their own. These results provide a potential mechanism for the evaporation resistance of the lipid layer. In addition, the results serve as a base for the future development of improved dry eye treatments and other applications where the evaporation of water represents a significant challenge.

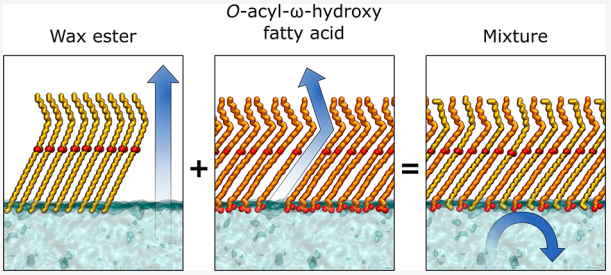

KEYWORDS: *Biophysics, Dry eye disease, Lipid, Evaporation resistance, Ocular surface, Self-assembly, Tear film lipid layer, Monolayer*

Dry eye disease (DED) is a prevalent ocular surface disease that constitutes a significant public health concern and a considerable societal economic burden.[1] While prevalent, the incidence of DED is expected to increase further in the future due to the connection between dry eye risk factors[1] and current global trends such as the aging population and the modern multiscreen lifestyle. The search for improved tools to combat the main pathological mechanisms of DED is ongoing. A major contributor to DED is the excessive evaporation of aqueous tear fluid, which causes tear film instability.[2,3] However, currently, effective evaporation resistant treatments are limited. In healthy eyes, the thin tear film lipid layer (TFLL) secreted by the Meibomian glands on the tear film surface stabilizes the entire tear film by suppressing the evaporation of water from the underlying aqueous tear fluid. This ability is compromised in dry eye patients, although the underlying factors are poorly understood.[4,5] The reasons for these shortcomings are related to the complex composition of the TFLL, which features 200−500 different lipid species from a variety of lipid classes.[6−8] Nevertheless, lipidomic studies on DED patients,[9−12] transgenic mouse studies,[13−15] and characterization of the biophysical properties of individual TFLL lipid species[16−21] have implicated that *O*-acyl-ω-hydroxy fatty acids (OAHFAs) and wax esters (WEs) may be central lipid classes with respect to evaporation resistance. However, the interactions between OAHFAs and WEs and their significance for tear film evaporation resistance have not been previously addressed.

To improve the mechanistic understanding of the TFLL function and to provide the first step toward improved solutions for dry eye patients, we set out to study the molecular level structure of films composed of OAHFAs and WEs and its correlation to evaporation resistance. As part of our experimental design, Langmuir monolayer techniques were used to study the self-assembly and evaporation resistance of OAHFAs and WEs on the aqueous interface, and wide-angle X-ray scattering (WAXS) was used to address their molecular packing in more detail. Instead of using the complex TFLL lipid species, which are expensive to produce due to the multistep synthetic routes and therefore not well suited for treatment applications, we opted to use model compounds that are either commercially available or can be prepared on an industrial scale by efficient and short processes. The following molecules were used: 20-oleoyloxy-eicosanoic acid (20-OAHFA), as a representative of a polar TFLL lipid,[18] and arachidyl oleate (AO) and behenyl oleate (BO), as representatives of nonpolar WEs (Figure 1).

We have previously studied the behavior and evaporation resistance of the 20-OAHFA alone,[18] and the WEs were chosen based on their melting points (33 °C for AO, 38 °C for BO),[16] which are slightly below and above the temperature of the ocular surface. Pure WEs have been found to resist

Received: June 24, 2021
Revised: August 26, 2021
Published: September 1, 2021

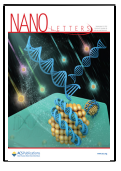

https://doi.org/10.1021/acs.nanolett.1c02475
Nano Lett. 2021, 21, 7676−7683

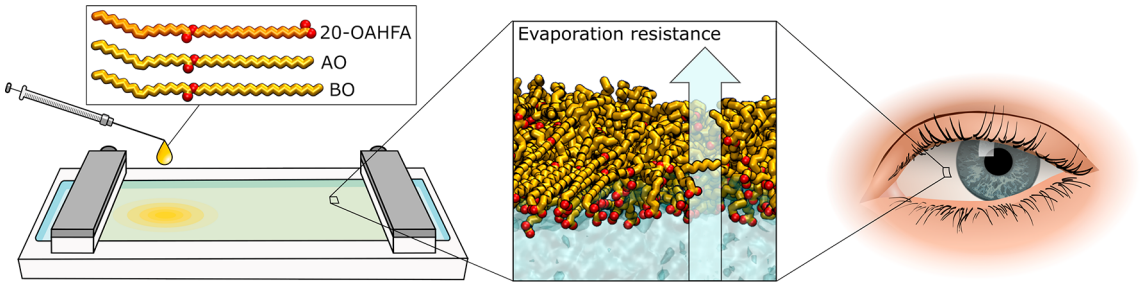

Figure 1. Langmuir trough setup used to study the organization and evaporation resistance of lipid mixtures is presented on the right. The relationship to dry eye is represented on the right. Molecular structures: *O*-acyl-ω-hydroxy fatty acid carbon chains are shown in orange, wax ester carbon chains are shown in yellow, and oxygen atoms are depicted in red. Hydrogen atoms are not shown.

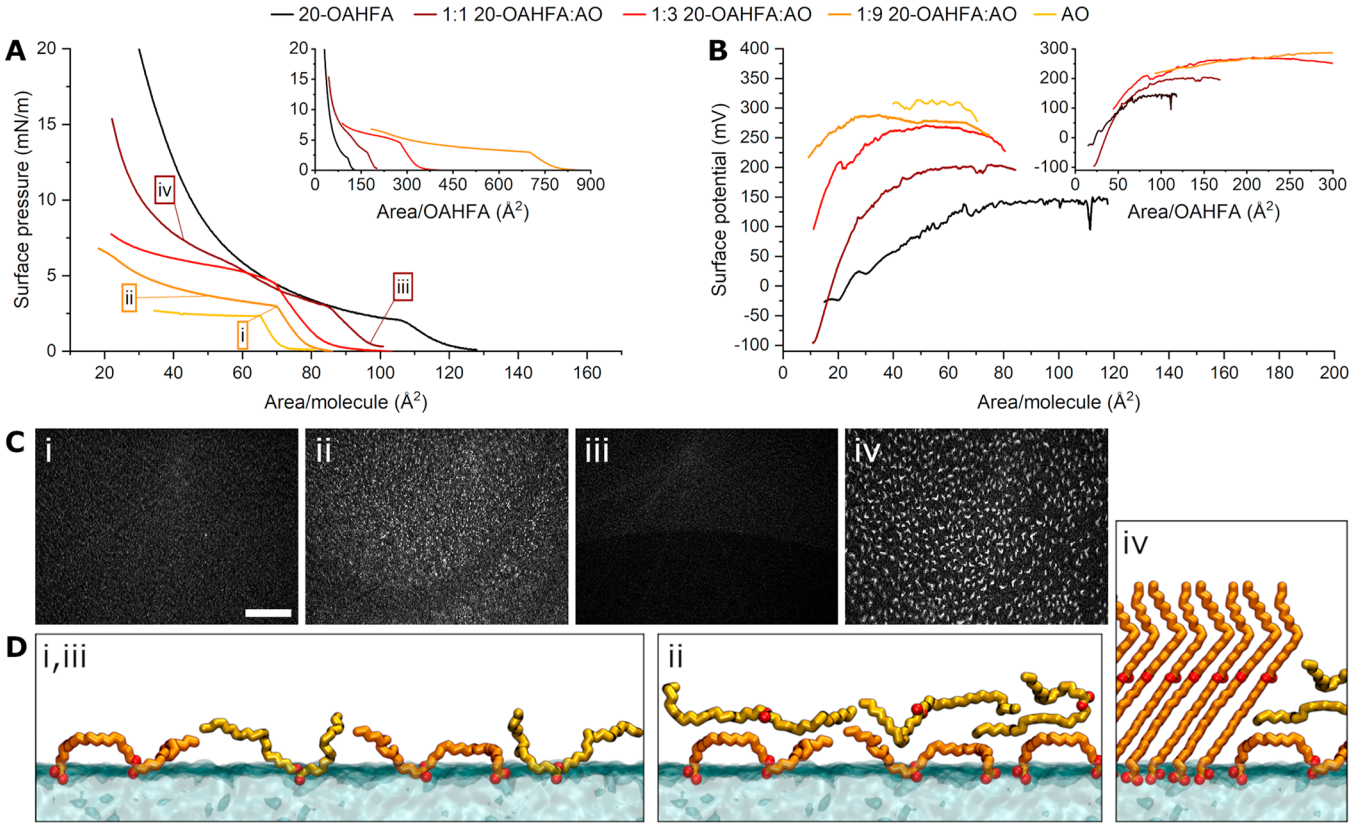

Figure 2. (A) Surface pressure and (B) surface potential isotherms of 20-OAHFA:AO mixtures, with (C) corresponding BAM images. The results are shown with respect to the total number of molecules (left) and the number of OAHFA molecules (right). The scale bar depicts 500 μm.(D) Schematic representation of the molecular organization of the films. Selected images correspond to the following conditions: (i) Mixed liquid monolayer of 20-OAHFA and AO, (ii) collapse of AO on the monolayer surface, (iii) coexistence of gas and liquid monolayer phases, and (iv) formation of solid monolayer domains by 20-OAHFA with overlying AO.

evaporation at temperatures close to their melting point,[16] but it is not known if the evaporation resistance of the tear film lipid mixtures has similar temperature dependency.

We began our investigations on OAHFA:WE mixtures by studying their behavior using Langmuir monolayer techniques. In our experimental setup, phosphate-buffered saline (PBS) was employed as a model for the aqueous tear fluid and maintained at physiological temperature (35 °C).[22] The lipid species and mixtures were administered onto the aqueous layer, and the properties of the films were analyzed by measuring the surface pressure and surface potential isotherms over compression/expansion cycles with further imaging by Brewster angle microscopy (BAM). This experimental setup mimics the conditions residing at the ocular surface and provides a good model for the lipid layer residing on the surface of the tear film. It can also simulate the changes occurring during a blink of the eye, although the dynamics of the compression and expansion are slower than those during natural blinking, and potential effects related to the flow of aqueous tear fluid are not accounted for.

Initially mixed films of 20-OAHFA and AO were studied. In their pure form, both the 20-OAHFA and AO formed liquid monolayers, with surface pressure lift-off areas occurring at 140 and 70 Å^2/molecule, respectively (Figure 2A). The difference in the mean molecular area reflects the distinct organization of these molecules at the aqueous interface. At low surface pressures, the amphiphilic 20-OAHFA lies flat on the aqueous surface, presumably through anchoring effects caused by both

https://doi.org/10.1021/acs.nanolett.1c02475
Nano Lett. 2021, 21, 7676−7683

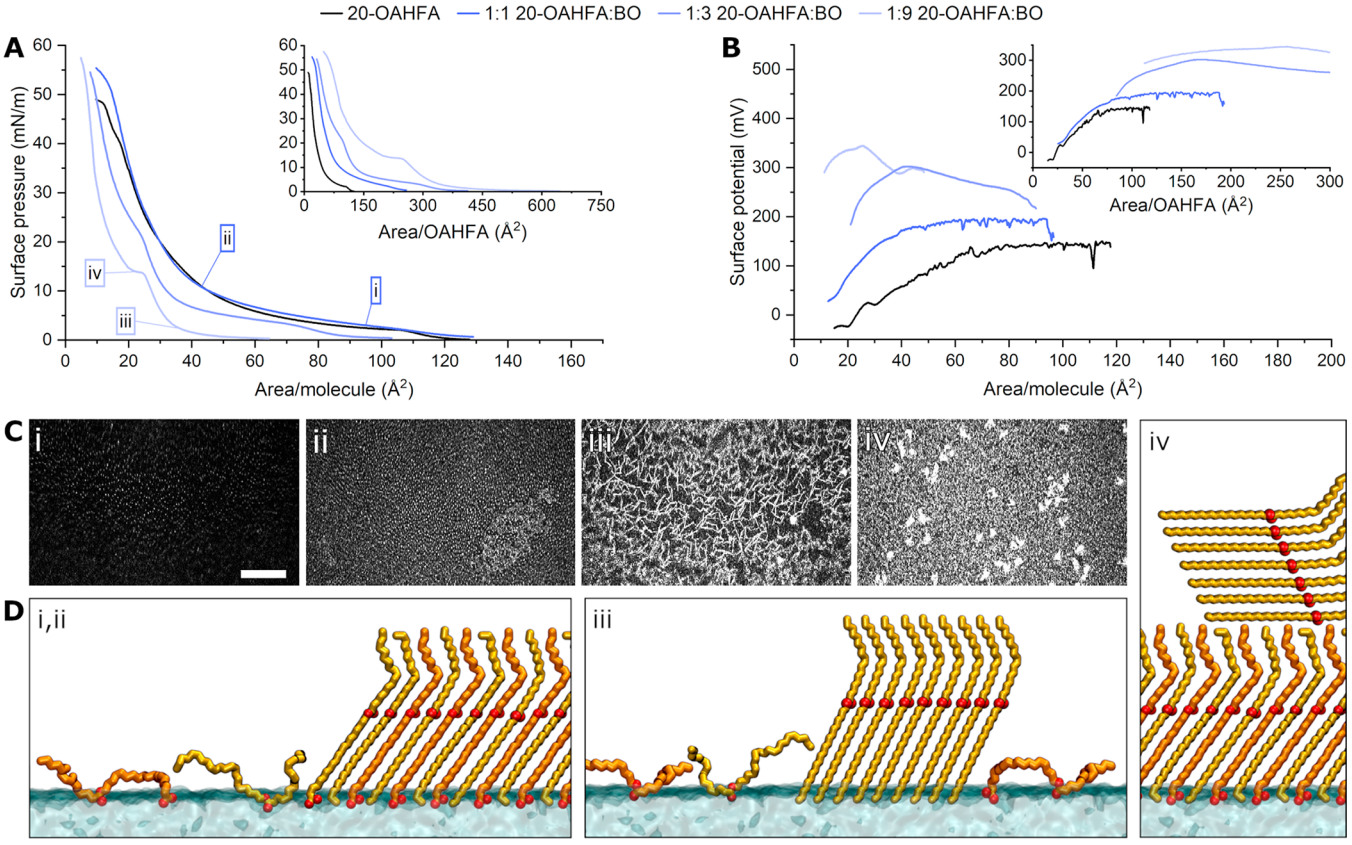

Figure 3. (A) Surface pressure and (B) surface potential isotherms of 20-OAHFA:BO mixtures, with (C) corresponding BAM images of the mixtures. The scale bar depicts 500 μm. (D) Schematic representation of the molecular organization of the 20-OAHFA:BO mixed films during compression. Selected images correspond to the following conditions: (i,ii) Formation of mixed solid monolayer domains of 20-OAHFA:BO, (iii) excess BO not mixed in the monolayer remains as solid aggregates, and (iv) solid mixed monolayer with excess BO aggregates collapsed on the monolayer surface.

the carboxylic acid and the carbonyl groups.[18] AO, on the contrary, lacks the carboxylic acid headgroup and is, as a result, only weakly oriented toward the aqueous interface under similar conditions.[19,20,23] Upon compression, the 20-OAHFA underwent a phase transition to a solid monolayer at 2 mN/m surface pressure. This shift in physical properties stemmed from a change in the organization of the molecules at the aqueous interface. At 2 mN/m the 20-OAHFA adopted a perpendicular "upright" orientation (Figure 2D, iv), presumably with the carboxylic acid headgroup anchored in the aqueous layer, as indicated by the plateau in the surface pressure isotherm and a decrease in the surface potential.[18] In contrast, the lack of a strong anchoring group in AO led to film collapse at a similar surface pressure, observed as plateaus in the surface pressure and surface potential isotherms, similar to the findings reported in previous reports on WE monolayers.[19,20,23]

In the exploration of the properties of 20-OAHFA:AO mixtures, the natural composition of tear film lipids was accounted for. In the TFLL, the proportion of OAHFAs and WEs is approximately 1:9.[6,7,24] To address the behavior that takes place in the natural TFLL, and in states substantially deviating from it, mixtures with increasing proportions of AO (20-OAHFA:AO-ratios: 1:1, 1:3, and 1:9) were investigated. In mixed films of 20-OAHFA and AO, the mean molecular area and the mean molecular dipole moment calculated from the surface potential at surface pressure lift-off were directly proportional to the ratio of the two components, indicating that the 20-OAHFA and AO were ideally miscible in the liquid monolayer phase (Figure 2A,B, Supporting Figure 2). Upon compression of the mixed films, the AO collapsed as droplets on top of the monolayer at low surface pressures (3−5 mN/m), as verified by the appearance of bright droplets in the BAM images (Figure 2C, i,ii) and plateaus in the surface pressure and potential isotherms (Figure 2A,B). Upon film expansion, however, the collapsed AO reintegrated into the monolayer. 20-OAHFA remained in the monolayer, shown by the surface pressure isotherms relative to the surface area/OAHFA approaching that of pure 20-OAHFA upon compression. A decrease in surface potential similar to that of pure 20-OAHFA was also observed, with a plateau at an area of 20 Å^2/OAHFA. At further compression, approaching the surface pressure values of the tear film (27−31 mN/m),[25] the 20-OAHFA residing in the monolayer formed a solid monolayer phase, observed as bright domains with a crystalline appearance in the BAM images (Figure 2C, iv). These results were in line with our recent findings on OAHFA:cholesteryl ester (CE) mixtures.[21] In more detail, the formation of the solid monolayer phase was unaffected by the presence of the varying amounts of AO. Moreover, measuring the evaporation resistance of 20-OAHFA:AO mixtures (Supporting Figure 3) showed that the evaporation resistance was solely governed by the 20-OAHFA. This was evident because the mixtures resisted evaporation only when the surface area/OAHFA was 20−25 Å^2 or smaller, that is, when 20-OAHFA adopted a solid monolayer phase. In addition, the maximum evaporation

https://doi.org/10.1021/acs.nanolett.1c02475
Nano Lett. 2021, 21, 7676−7683

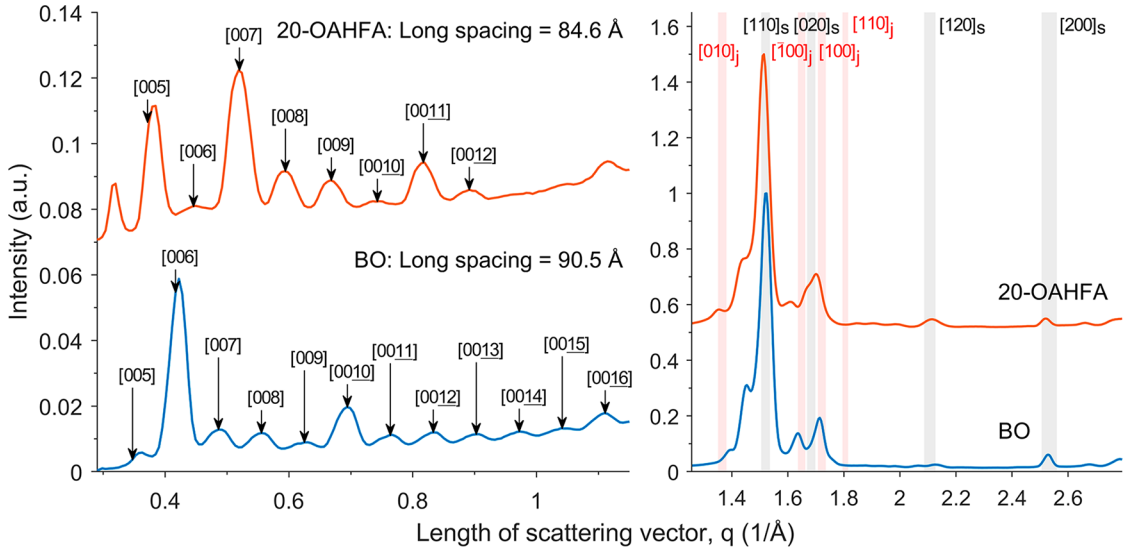

Figure 4. Wide-angle X-ray scattering results of bulk 20-OAHFA and BO samples. Left: Smaller scattering angles with diffraction peak orders from long spacing shown. Right: Peaks at larger scattering angles corresponding to the side spacings. Reflections observed in saturated wax esters[29,30] are shown in gray and labeled with subscript "s", and reflections observed in jojoba wax esters[31] are shown in red and labeled with subscript "j".

resistance reached similar levels as those for the pure 20-OAHFA (3−6 s/cm).[18]

The TFLL is typically depicted as a thin, liquid, or liquid-crystalline layer of nonpolar lipids, with a monolayer of amphiphilic lipids at the aqueous tear film surface. 20-OAHFA:AO mixtures formed a similar structure when compressed, but the AO that collapsed on top of the polar 20-OAHFA monolayer did not provide evaporation resistance, even though the fully compressed films contained enough lipids to reach a total thickness of ∼40 nm, which is close to the estimated TFLL thickness.[26,27] Taken together with the similar results on OAHFA:CE mixtures,[21] these results suggest that it is unlikely that a liquid or liquid-crystalline layer of nonpolar lipids provides significant evaporation resistance in the TFLL. In other words, it seemed likely in this stage that the origin of TFLL evaporation resistance, one of the main factors contributing to tear film stability, would stem single-handedly from the condensed layer of polar lipids residing at the aqueous interface. Therefore, we wanted to address the interplay and properties arising from a combination of our model OAHFA and nonpolar lipids that adopt a solid phase under physiological conditions.

On the basis of previous studies on WEs,[16,20] BO was deemed to be a good lipid to represent tear film WEs with higher melting points. It is structurally similar to AO (slight increase in chain length) and has similar overall properties, with the exception of its slightly higher melting/boiling points. However, these differences are considerable when viewed from a biophysical perspective. The slight increase in the melting point entails that BO exists in the solid state under physiological conditions, in contrast with AO, which exists in the liquid state. Because of this, pure BO did not spread on the aqueous surface at 35 °C but instead formed solid aggregates; therefore, reproducible isotherms could not be obtained with pure BO. However, to determine how the surface organization of BO was affected by 20-OAHFA, a number of 20-OAHFA:BO mixtures (3:1, 2:1, 3:2, 1:1, 1:3, 1:9) were prepared, and their properties were assessed.

In the 1:1 20-OAHFA:BO mixture, a homogeneous liquid monolayer was initially observed at low surface pressures, indicating that the surfactant properties of the 20-OAHFA induced the spreading of BO. During compression, a liquid-to-solid phase transition (Figure 3C, i,ii) occurred, similar to that for pure 20-OAHFA, accompanied by a plateau in the surface pressure at 2 to 3 mN/m and followed by a steep increase in the surface pressure to >50 mN/m and a collapse at a mean molecular area of ∼20 Å^2/molecule (Figure 3A). Also, surface potential isotherms exhibited a plateau at the same molecular area but a higher surface potential than pure 20-OAHFA (Figure 3B). This contrasts with 20-OAHFA:AO mixtures and other nonpolar lipids studied previously,[21] where the mean molecular area of the film decreased compared with that of pure 20-OAHFA at high surface pressures due to the collapse of the nonpolar component from the film. In the 1:1 20-OAHFA:BO mixture, the mean molecular area was close to pure 20-OAHFA, even at high surface pressures, indicating that BO occupied a similar area per molecule in the film as 20-OAHFA. This suggests that BO did not collapse on top of the polar lipid layer but was instead integrated into the solid monolayer, even at high surface pressures corresponding to the natural tear fluid (Figure 3D, i,ii).[25]

At lower 20-OAHFA:BO ratios (1:3 to 1:9), the BAM images showed that solid aggregates, likely consisting of excess BO not mixed into the monolayer phase, formed already at low surface pressures (Figure 3C, iii). Upon compression, BO and 20-OAHFA self-assembled to a solid monolayer at the aqueous interface, and the solid BO aggregates were pushed on top of the monolayer (Figure 3C, iv). The collapse of excess BO from the surface was accompanied by a second plateau in the surface pressure isotherms at 14−22 mN/m. This indicated that there is a limit for BO integration in the amphiphilic monolayer, and after the threshold is reached, the remaining BO molecules display a similar behavior as BO in its pure form. To explore the boundaries of the behavior from a TFLL perspective, we performed compression−expansion cycles to simulate the changes occurring during an eye blink. The solid aggregates formed by superfluous BO did not respread as the film was expanded, as seen from the surface pressure isotherm expansion cycles (Supporting Figure 4). Altogether, we arrived at the conclusion that coassembly of 20-OAHFA and BO in

https://doi.org/10.1021/acs.nanolett.1c02475
Nano Lett. 2021, 21, 7676−7683

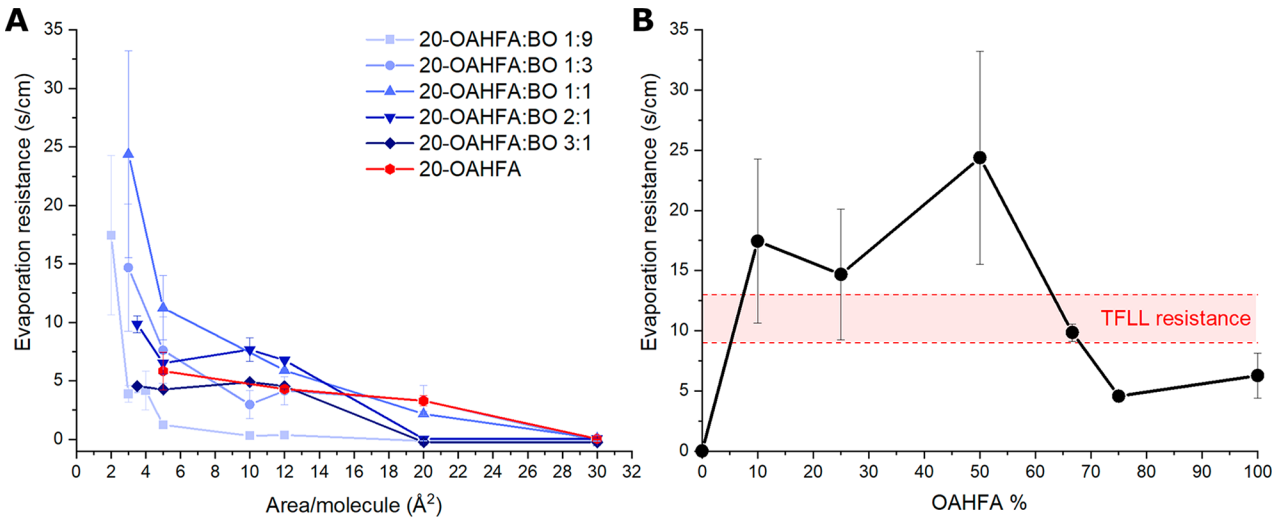

Figure 5. (A) Evaporation resistance of 20-OAHFA/BO mixtures as a function of the mean molecular area. (B) Evaporation resistance of fully compressed films as a function of the film composition (mol percent of 20-OAHFA), with TFLL evaporation resistance[37,38] as a reference. Error bars depict the standard deviation.

the amphiphilic sublayer at the aqueous interface occurs at a ratio of approximately 1:1 of both components.

These results demonstrate the joint self-assembly of a nonpolar WE and a polar OAHFA into a mixed solid monolayer at the aqueous interface. In the context of the TFLL, this suggests that WEs can integrate into the organized amphiphilic sublayer at the aqueous interface. Whereas such experimental evidence has been lacking up until now, a preliminary simulation study had predicted that the amphiphilic sublayer of the TFLL may contain up to 30% of nonpolar WEs and CEs.[28] However, it appears that specific interactions are required for a mixture of nonpolar and polar lipids to form a stable condensed layer at the aqueous interface; therefore, it is unlikely that the majority of nonpolar lipid species present in the TFLL would integrate into the polar sublayer. The 20-OAHFA:BO mixture is an example of this and provides a sound platform for identifying other lipid species with similar properties in the TFLL.

Realizing that BO and 20-OAHFA appeared to form a mixed condensed monolayer at the aqueous interface, we investigated the molecular packing of 20-OAHFA and BO in more detail using WAXS (Figure 4). On the basis of the reflections in the WAXS patterns, 20-OAHFA and BO were found to exhibit very similar crystalline structures in bulk form at room temperature. The long spacing values observed (84.6 and 90.5 Å for 20-OAHFA and BO, respectively, with a 0.3 Å error limit) were significantly larger than those previously reported for saturated WEs,[29,30] suggesting bilayer-type packing for both lipids in their bulk form. In the case of 20-OAHFA, the bilayer-type packing likely includes hydrogen bonding between the carboxylic acid head groups of adjacent lamellae. The reflections arising from the short spacing suggested that the methylene subcell packing of 20-OAHFA and BO is markedly different from the previously reported results for both saturated WEs[29,30] and unsaturated jojoba WEs,[31] thus indicating a distinct lateral packing. The short spacing reflections were very similar for both 20-OAHFA and BO, which is supportive of the idea that these lipids may form a mixed solid phase at the aqueous interface. That being said, it is simultaneously important to note that differences may occur between the packing in bulk states and the ones residing at the aqueous interface.

With a detailed understanding of the organization and behavior of these mixtures uncovered, we continued by studying the effects of intercalating WEs on the evaporation resistance, an essential factor related to tear film stability. The solid monolayer formed by the coassembly of BO and 20-OAHFA species had a drastic effect on the evaporation resistance, with the evaporation resistance increasing significantly when 50−90% of BO was included in the film (Figure 5). The evaporation resistance for these mixtures was found to be as high as 24 s/cm, in contrast with the modest evaporation resistance observed for the pure 20-OAHFA,[18] 20-OAHFA:CE,[21] and 20-OAHFA:AO mixtures (3−6 s/cm). This evaporation resistance is remarkable and exceeds those previously reported for lipid monolayers,[32] to the best of our knowledge. In previous work, mixing lipid species with different structures has often led to a loss of evaporation resistance, such as in the case of cholesterol and octadecanol[33] or L-α-phosphatidylcholine and BO.[34] However, mixing lipids with similar structures and chain lengths has been shown to retain evaporation-resistant properties[35] or even improve the evaporation resistance at specific compositions.[36] The evaporation resistances of the 20-OAHFA:BO mixtures were also higher than the evaporation resistance estimated for the TFLL (9−13 s/cm)[37,38] and would correspond to a significant (up to 95%) reduction in the evaporation rate from the ocular surface under ambient natural conditions.[39]

When considering the mechanism behind the improved evaporation resistance of 20-OAHFA:BO we suspected that the intercalation of BO molecules in the monolayer would allow a more tightly packed organization by reducing the repulsion caused by the negatively charged carboxylate head groups in neighboring 20-OAHFAs when compressed to the perpendicular conformation. To explore this hypothesis, we measured the evaporation resistance of the pure 20-OAHFA employing nonphysiological conditions with an acidic and basic aqueous subphase (pH 2 or 10; Supporting Figure 5). Through this simple experimental setup, we sought to uncover the effect of a protonated versus charged headgroup on the evaporation-resistant properties. To our surprise, our initial

https://doi.org/10.1021/acs.nanolett.1c02475
Nano Lett. 2021, 21, 7676−7683

thoughts were proven wrong. In fact, at high pH, with a maximum number of head groups in the carboxylate form, the 20-OAHFA exhibited an evaporation resistance (20 s/cm) similar to that of the 20-OAHFA:BO mixtures, whereas the protonated form displayed an evaporation resistance reminiscent to that of the 20-OAHFA under physiological conditions. The charged headgroup therefore does not appear to hinder the formation of a densely packed solid monolayer but rather it increases the evaporation resistance. In light of these findings, understanding the effects of BO on the coassembly of the 20-OAHFA:BO solid monolayer requires further investigations. In this stage, it seems probable that the uniform crystallization or formation of larger crystallites requires either a large number of charged head groups or a tailored composition capable of balancing these properties through an appropriate nanoscale architecture. This would be in line with the current models available, which suggest that the passage of water molecules likely proceeds through domain boundaries or other imperfections in the film.[20,40]

To conclude, we set out to study the organization and properties of mixed OAHFA:WE films to shed light on the interplay between these lipid species and their respective roles in the TFLL. Surprisingly, WEs existing in the solid state under physiological conditions were capable of forming a mixed condensed monolayer with OAHFAs, and such a monolayer exhibited very high evaporation resistance. Together with our previous studies on pure OAHFAs[18,41] and OAHFA:CE mixtures,[21] our results support the conclusion that the amphiphilic sublayer, which resides at the interface between the aqueous tear film and the lipid layer, is responsible for the evaporation-resistant properties of the TFLL. However, the integration of nonpolar WEs into this interfacial layer is likely to further increase the evaporation resistance, as demonstrated here. Whereas the results were obtained with model compounds under carefully controlled experimental conditions, they provide a solid basis for identifying TFLL lipid species, which may integrate into the amphiphilic sublayer under natural conditions.

In addition, these results can aid in the development of solutions to global challenges in which the evaporation of water presents a significant obstacle. First off, they could be utilized to develop new treatments for DED that would function by restoring the antievaporative function of the TFLL, thereby providing a unique solution for targeting the central tear film instability defect. Whereas it is still too early to draw definite conclusions, we are certain that an improved dry eye treatment based on natural-like lipid components would be welcomed by the hundreds of millions of people who suffer from this disease on a global scale.[1] Second, similar mixtures may be used to mitigate the evaporation of water from artificial lakes and reservoirs, which is becoming an increasing challenge due to the global climate change.[42−44]

■ ASSOCIATED CONTENT

Supporting Information

The Supporting Information is available free of charge at https://pubs.acs.org/doi/10.1021/acs.nanolett.1c02475.

Additional experimental details and results including materials and methods, mean molecular dipole moments and evaporation resistance of 20-OAHFA:AO mixtures, compression−expansion cycles of 20-OAHFA:BO films, and the effect of the subphase pH on the 20-OAHFA evaporation resistance (PDF)

■ AUTHOR INFORMATION

Corresponding Authors

Filip S. Ekholm − *Department of Chemistry, University of Helsinki, FI-00014 Helsinki, Finland;* orcid.org/0000-0002-4461-2215; Email: filip.ekholm@helsinki.fi

Riku O. Paananen − *Ophthalmology, University of Helsinki and Helsinki University Hospital, FI-00290 Helsinki, Finland; Department of Chemistry, University of Helsinki, FI-00014 Helsinki, Finland;* orcid.org/0000-0002-2703-6359; Email: riku.o.paananen@helsinki.fi

Authors

Tuomo Viitaja − *Ophthalmology, University of Helsinki and Helsinki University Hospital, FI-00290 Helsinki, Finland; Department of Chemistry, University of Helsinki, FI-00014 Helsinki, Finland*

Jukka Moilanen − *Ophthalmology, University of Helsinki and Helsinki University Hospital, FI-00290 Helsinki, Finland*

Kirsi Johanna Svedström − *Department of Physics, University of Helsinki, FI-00014 Helsinki, Finland*

Complete contact information is available at: https://pubs.acs.org/10.1021/acs.nanolett.1c02475

Funding

The authors are grateful for the financial support from the Evald and Hilda Nissi Foundation, the Mary and Georg C. Ehrnrooth Foundation, the Vilho, Yrjö, and Kalle Väisälä Foundation, the Finnish Eye Foundation, the Swedish Cultural Foundation, the Ruth and Nils-Erik Stenbäck Foundation, the Orion Research Foundation, the Eye and Tissue Bank Foundation, and the state research funding in Finland.

Notes

The authors declare the following competing financial interest(s): A patent application (FI20215505) related to this manuscript has been filed by R.O.P., T.V., J.M., and F.S.E.

■ ACKNOWLEDGMENTS

The authors thank BSc. student Saga Grönfors (Ophthalmology, University of Helsinki and Helsinki University Hospital/Department of Chemistry, University of Helsinki) for laboratory assistance.

■ ABBREVIATIONS

BAM, Brewster angle microscope; DED, dry eye disease; OAHFA, *O*-acyl-ω-hydroxy-fatty acid; TFLL, tear film lipid layer; WAXS, wide-angle X-ray scattering; WE, wax ester.

■ REFERENCES

(1) Stapleton, F.; Alves, M.; Bunya, V. Y.; Jalbert, I.; Lekhanont, K.; Malet, F.; Na, K.; Schaumberg, D.; Uchino, M.; Vehof, J.; Viso, E.; Vitale, S.; Jones, L. TFOS DEWS II Epidemiology Report. *Ocul Surf.* **2017**, *15*, 334−365.

(2) Craig, J. P.; Nichols, K. K.; Akpek, E. K.; Caffery, B.; Dua, H. S.; Joo, C.; Liu, Z.; Nelson, J. D.; Nichols, J. J.; Tsubota, K.; Stapleton, F. TFOS DEWS II Definition and Classification Report. *Ocul Surf.* **2017**, *15*, 276−283.

(3) Jones, L.; Downie, L. E.; Korb, D.; Benitez-Del-Castillo, J. M.; Dana, R.; Deng, S. X.; Dong, P. N.; Geerling, G.; Hida, R. Y.; Liu, Y.; Seo, K. Y.; Tauber, J.; Wakamatsu, T. H.; Xu, J.; Wolffsohn, J. S.;

Craig, J. P. TFOS DEWS II Management and Therapy Report. *Ocul Surf.* **2017**, *15*, 575−628.
(4) Willcox, M. D. P.; Argüeso, P.; Georgiev, G. A.; Holopainen, J. M.; Laurie, G. W.; Millar, T. J.; Papas, E. B.; Rolland, J. P.; Schmidt, T. A.; Stahl, U.; Suarez, T.; Subbaraman, L. N.; Uçakhan, O. Ö.; Jones, L. TFOS DEWS II Tear Film Report. *Ocul Surf.* **2017**, *15*, 366−403.
(5) Georgiev, G. A.; Eftimov, P.; Yokoi, N. Structure-Function Relationship of Tear Film Lipid Layer: A contemporary Perspective. *Exp. Eye Res.* **2017**, *163*, 17−28.
(6) Brown, S. H.; Kunnen, C. M.; Duchoslav, E.; Dolla, N. K.; Kelso, M. J.; Papas, E. B.; Lazon de la Jara, P.; Willcox, M. D.; Blanksby, S. J.; Mitchell, T. W. A Comparison of Patient Matched Meibum and Tear Lipidomes. *Invest. Ophthalmol. Visual Sci.* **2013**, *54*, 7417−7424.
(7) Lam, S. M.; Tong, L.; Duan, X.; Petznick, A.; Wenk, M. R.; Shui, G. Extensive Characterization of Human Tear Fluid Collected using Different Techniques Unravels the Presence of Novel Lipid Amphiphiles. *J. Lipid Res.* **2014**, *55*, 289−298.
(8) Chen, J.; Green, K. B.; Nichols, K. K. Quantitative Profiling of Major Neutral Lipid Classes in Human Meibum by Direct Infusion Electrospray Ionization Mass Spectrometry. *Invest. Ophthalmol. Visual Sci.* **2013**, *54*, 5730−5753.
(9) Lam, S. M.; Tong, L.; Yong, S. S.; Li, B.; Chaurasia, S. S.; Shui, G.; Wenk, M. R. Meibum Lipid Composition in Asians with Dry Eye Disease. *PLoS One* **2011**, *6*, No. e24339.
(10) Lam, S. M.; Tong, L.; Duan, X.; Acharya, U. R.; Tan, J. H.; Petznick, A.; Wenk, M. R.; Shui, G. Longitudinal Changes in Tear Fluid Lipidome Brought about by Eyelid-Warming Treatment in a Cohort of Meibomian Gland Dysfunction. *J. Lipid Res.* **2014**, *55*, 1959−1969.
(11) Lam, S. M.; Tong, L.; Reux, B.; Duan, X.; Petznick, A.; Yong, S. S.; Khee, C. B. S.; Lear, M. J.; Wenk, M. R.; Shui, G. Lipidomic Analysis of Human Tear Fluid Reveals Structure-Specific Lipid Alterations in Dry Eye Syndrome. *J. Lipid Res.* **2014**, *55*, 299−306.
(12) Butovich, I. A.; Wojtowicz, J. C.; Molai, M. Human Tear Film and Meibum. very Long Chain Wax Esters and (O-Acyl)-Omega-Hydroxy Fatty Acids of Meibum. *J. Lipid Res.* **2009**, *50*, 2471−2485.
(13) Sassa, T.; Tadaki, M.; Kiyonari, H.; Kihara, A. Very Long-Chain Tear Film Lipids Produced by Fatty Acid Elongase ELOVL1 Prevent Dry Eye Disease in Mice. *FASEB J.* **2018**, *32*, 2966−2978.
(14) Miyamoto, M.; Sassa, T.; Sawai, M.; Kihara, A. Lipid Polarity Gradient Formed by ω-Hydroxy Lipids in Tear Film Prevents Dry Eye Disease. *eLife* **2020**, *9*, No. e53582.
(15) Butovich, I. A.; Wilkerson, A.; Bhat, N.; McMahon, A.; Yuksel, S. On the Pivotal Role of Elovl3/ELOVL3 in Meibogenesis and Ocular Physiology of Mice. *FASEB J.* **2019**, *33*, 10034−10048.
(16) Rantamäki, A. H.; Wiedmer, S. K.; Holopainen, J. M. Melting Points–the Key to the Anti-Evaporative Effect of the Tear Film Wax Esters. *Invest. Ophthalmol. Visual Sci.* **2013**, *54*, 5211−5217.
(17) Schuett, B. S.; Millar, T. J. An Investigation of the Likely Role of (O-Acyl) Ω-Hydroxy Fatty Acids in Meibomian Lipid Films using (O-Oleyl) ω-Hydroxy Palmitic Acid as a Model. *Exp. Eye Res.* **2013**, *115*, 57−64.
(18) Bland, H. C.; Moilanen, J. A.; Ekholm, F. S.; Paananen, R. O. Investigating the Role of Specific Tear Film Lipids Connected to Dry Eye Syndrome: A Study on O-Acyl-ω-Hydroxy Fatty Acids and Diesters. *Langmuir* **2019**, *35*, 3545−3552.
(19) Paananen, R. O.; Rantamäki, A. H.; Holopainen, J. M. Antievaporative Mechanism of Wax Esters: Implications for the Function of Tear Fluid. *Langmuir* **2014**, *30*, 5897−5902.
(20) Paananen, R. O.; Javanainen, M.; Holopainen, J. M.; Vattulainen, I. Crystalline Wax Esters Regulate the Evaporation Resistance of Tear Film Lipid Layers Associated with Dry Eye Syndrome. *J. Phys. Chem. Lett.* **2019**, *10*, 3893−3898.
(21) Paananen, R. O.; Viitaja, T.; Olżyńska, A.; Ekholm, F. S.; Moilanen, J.; Cwiklik, L. Interactions of Polar Lipids with Cholesteryl Ester Multilayers Elucidate Tear Film Lipid Layer Structure. *Ocular Surf.* **2020**, *18*, 545−553.
(22) Shah, A. M.; Galor, A. Impact of Ocular Surface Temperature on Tear Characteristics: Current Insights. *Clin Optom (Auckl)* **2021**, *13*, 51−62.
(23) Caruso, B.; Martini, M. F.; Pickholz, M.; Perillo, M. A. V-Shaped Molecular Configuration of Wax Esters of Jojoba Oil in a Langmuir Film Model. *Langmuir* **2018**, *34*, 7887−7898.
(24) Rohit, A.; Stapleton, F.; Brown, S. H. J.; Mitchell, T. W.; Willcox, M. D. P. Comparison of Tear Lipid Profile among Basal, Reflex, and Flush Tear Samples. *Optom Vis Sci.* **2014**, *91*, 1391−1395.
(25) Nagyová, B.; Tiffany, J. M. Components Responsible for the Surface Tension of Human Tears. *Curr. Eye Res.* **1999**, *19*, 4−11.
(26) King-Smith, P. E.; Hinel, E. A.; Nichols, J. J. Application of a Novel Interferometric Method to Investigate the Relation between Lipid Layer Thickness and Tear Film Thinning. *Invest. Ophthalmol. Visual Sci.* **2010**, *51*, 2418−2423.
(27) Bai, Y.; Ngo, W.; Nichols, J. J. Characterization of the Thickness of the Tear Film Lipid Layer using High Resolution Microscopy. *Ocul Surf.* **2019**, *17*, 356−359.
(28) Paananen, R.; Cwiklik, L. Using Molecular Dynamics Simulations to Build a Nanoscale in Silico Model of the Tear Film Lipid Layer. *Invest. Ophthalmol. Vis. Sci.* **2019**, *60*, 4177−4178.
(29) Kohlhaas, R. Röntgenographische Untersuchung Von Definierten Einkristallen Des Palmitinsäure-Cetylesters. *Z. Kristallogr. - Cryst. Mater.* **1938**, *98*, 418−438.
(30) Lutz, D. A.; Eddy, C. R.; Hunter, J. J. X-Ray Diffraction Study of some Normal Alkyl Esters of Long-Chain Acids. *Lipids* **1967**, *2*, 204−207.
(31) Bouzidi, L.; Li, S.; Di Biase, S.; Rizvi, S. Q.; Narine, S. S. Lubricating and Waxy Esters, I. Synthesis, Crystallization, and Melt Behavior of Linear Monoesters. *Chem. Phys. Lipids* **2012**, *165*, 38−50.
(32) Barnes, G. T. The Potential for Monolayers to Reduce the Evaporation of Water from Large Water Storages. *Agric. Water Manage.* **2008**, *95*, 339−353.
(33) McNamee, C. E.; Barnes, G. T.; Gentle, I. R.; Peng, J. B.; Steitz, R.; Probert, R. The Evaporation Resistance of Mixed Monolayers of Octadecanol and Cholesterol. *J. Colloid Interface Sci.* **1998**, *207*, 258−263.
(34) Rantamäki, A. H.; Javanainen, M.; Vattulainen, I.; Holopainen, J. M. Do Lipids Retard the Evaporation of the Tear Fluid? *Invest. Ophthalmol. Visual Sci.* **2012**, *53*, 6442−6447.
(35) La Mer, V. K.; Aylmore, L. A. G.; Healy, T. W. The Ideal Surface Behavior of Mixed Monolayers of Long-Chain n-Paraffinic Alcohols. *J. Phys. Chem.* **1963**, *67*, 2793−2795.
(36) Rao, Y. K.; Shah, D. O. Detection of Phase Transitions in Monolayers using Retardation of Evaporation of Water. *J. Colloid Interface Sci.* **1990**, *137*, 25−29.
(37) Iwata, S.; Lemp, M. A.; Holly, F. J.; Dohlman, C. H. Evaporation Rate of Water from the Precorneal Tear Film and Cornea in the Rabbit. *Invest. Ophthalmol.* **1969**, *8*, 613−619.
(38) Peng, C. -C.; Cerretani, C.; Li, Y.; Bowers, S.; Shahsavarani, S.; Lin, M. C.; Radke, C. J. Flow Evaporimeter to Assess Evaporative Resistance of Human Tear-Film Lipid Layer. *Ind. Eng. Chem. Res.* **2014**, *53*, 18130−18139.
(39) Cerretani, C. F.; Ho, N. H.; Radke, C. J. Water-Evaporation Reduction by Duplex Films: Application to the Human Tear Film. *Adv. Colloid Interface Sci.* **2013**, *197*−*198*, 33−57.
(40) Barnes, G. T. Permeation through Monolayers. *Colloids Surf., A* **1997**, *126*, 149−158.
(41) Viitaja, T.; Raitanen, J.; Moilanen, J.; Paananen, R. O.; Ekholm, F. S. The Properties and Role of O-Acyl-ω-Hydroxy Fatty Acids and Type I-St and Type II Diesters in the Tear Film Lipid Layer Revealed by a Combined Chemistry and Biophysics Approach. *J. Org. Chem.* **2021**, *86*, 4965−4976.
(42) Helfer, F.; Lemckert, C.; Zhang, H. Impacts of Climate Change on Temperature and Evaporation from a Large Reservoir in Australia. *J. Hydrol.* **2012**, *475*, 365−378.
(43) Althoff, D.; Rodrigues, L. N.; da Silva, D. D. Impacts of Climate Change on the Evaporation and Availability of Water in Small

https://doi.org/10.1021/acs.nanolett.1c02475
Nano Lett. 2021, 21, 7676−7683

Reservoirs in the Brazilian Savannah. *Clim. Change* **2020**, *159*, 215−232.
(44) Friedrich, K.; Grossman, R. L.; Huntington, J.; Blanken, P. D.; Lenters, J.; Holman, K. D.; Gochis, D.; Livneh, B.; Prairie, J.; Skeie, E.; Healey, N. C.; Dahm, K.; Pearson, C.; Finnessey, T.; Hook, S. J.; Kowalski, T. Reservoir Evaporation in the Western United States: Current Science, Challenges, and Future Needs. *Bull. Am. Meteorol. Soc.* **2018**, *99*, 167−187.

https://doi.org/10.1021/acs.nanolett.1c02475
Nano Lett. 2021, 21, 7676−7683